

Article

The Influence of Polymeric Sealing Treatment on the Wear Performance of PEO Coating Deposited on AZ31 Mg Alloy

Qun Wang ^{1,*}, Sisi Tu ¹, Yuqin Rao ¹ and Ramachandran Chidambaram Seshadri ²

¹ College of Materials Science and Engineering, Hunan University, Changsha 410082, China; tusihnu@163.com (S.T.); ryuki@hnu.edu.cn (Y.R.)

² Department of Materials Science and Engineering, The State University of New York at Stony Brook, New York, NY 11794, USA; csrn1@gmail.com

* Correspondence: wangqun@hnu.edu.cn

Abstract: A plasma electrolytic oxidation (PEO) coating fabricated on AZ31 Mg alloy was sealed with polymeric sealant. The sealant penetrated into the PEO coating and filled the micropores and microcracks of the coating. The effect of the sealant treatment on the sliding wear behavior of the PEO coating was investigated by systematically varying the axial wear loads applied onto the unsealed and sealed PEO coatings. The results of the sliding wear tests revealed that the polymeric sealing treatment enhanced the wear resistance of the Mg-based PEO coating by reducing the wear rate and by improving the load-bearing capacity.

Keywords: ceramics; polymers; metals and alloys; sliding wear; sealing; PEO



Citation: Wang, Q.; Tu, S.; Rao, Y.; Chidambaram Seshadri, R. The Influence of Polymeric Sealing Treatment on the Wear Performance of PEO Coating Deposited on AZ31 Mg Alloy. *Coatings* **2022**, *12*, 182. <https://doi.org/10.3390/coatings12020182>

Academic Editors: Anton Ficaí and Monica Santamaria

Received: 8 December 2021

Accepted: 28 January 2022

Published: 30 January 2022

Publisher's Note: MDPI stays neutral with regard to jurisdictional claims in published maps and institutional affiliations.



Copyright: © 2022 by the authors. Licensee MDPI, Basel, Switzerland. This article is an open access article distributed under the terms and conditions of the Creative Commons Attribution (CC BY) license (<https://creativecommons.org/licenses/by/4.0/>).

1. Introduction

Mg and its alloys are extensively utilized in many fields due to its lightweight and outstanding properties [1,2]. However, it has long been a concern to provide surface protection for Mg and its alloys to prolong their service life since they are prone to wear and corrosion. Plasma electrolytic oxidation (PEO) has been used to improve the wear and corrosion resistances of the Mg, Al, Ti and other alloys [3–6]. The surfaces of the Mg-based PEO coatings are mainly composed of Mg-based oxides and its compounds, which possess higher hardness than the Mg alloy substrates. Micropores and microcracks are usually present in the Mg-based PEO coatings, which limit their wear and corrosion resistances [7,8]. These microdefects cannot be completely eliminated by optimizing the parameters of the PEO process or the composition of electrolyte [9,10]. Therefore, various sealants and resultant sealing treatments are employed to seal these microdefects (pores and cracks), resulting in the improvement of the properties of the Mg-based PEO coatings. There are two kinds of commonly used sealants, namely, organic and inorganic sealants. Organic sealants include epoxy [11,12], polytetrafluoroethylene [13], epoxy-based organosilane [14], octodecylphosphate acid [15], and paraffin wax [16]. The inorganic sealants encompass silane [12], phosphate, cerium and stannate-based salt solutions [15,17]. The sealing treatment process involves brushing [16], soaking [13,15,17,18], sol-gel infusion [19], hydrothermal routes [20], etc. Among the many methods, the polymeric sealing treatment is a simple, easy, low-cost and effective post-coating treatment to seal the surface of the Mg-based PEO coatings, which can significantly enhance their mechanical and corrosion properties [11,12,16]. However, the research on the sealing of Mg-PEO coatings were mainly focused on the improvement of corrosion resistance of the coatings only [11–20], and very little attention was paid to investigate its effect on wear properties [13]. A commercially available DIAMANT Dichtol WFT (1532) type sealant was chosen (main component: ketone), since it is a fast-curing capillary sealer that can impregnate micropores and hairline cracks without the need for vacuum or pressure. Hence, it is commonly applied onto thermal sprayed coatings, which results in an excellent sealing effect [21]. Furthermore, the sealant-infiltrated and cured

coating can provide exceptional chemical as well as temperature resistance. Therefore, in this work, this sealant with ketone as the main component was used to seal the AZ31 Mg–PEO coating, having similar pores and cracks as that of the thermal sprayed coatings to some extent. This investigation is mainly intended to explore the effect of sealing treatment on the sliding wear behavior of the AZ31 Mg–PEO coating.

2. Experiment

AZ31 Mg alloy specimens (wt%, Al 2.33, Zn 1.21, Mn 0.49, Si < 0.1, Fe < 0.005, Cu < 0.05, Ni < 0.005, and Mg balance) were used as substrates. The specimens were mounted, leaving an exposed area of 2 cm². The working surfaces were ground and polished before PEO treatment. The PEO coatings were formed in 12 g/L Na₂SiO₃·9H₂O + 10 g/L (NaPO₃)₆ + 1 g/L KOH + 30 mL/L glycerin solution, using a 15 kW pulsed power source (JCL-DL15, Chengdu Golden Creation Technology Co. Ltd., Chengdu, China). During the PEO process, a constant current setting (positive current: 0.4 A and negative current: 0.3 A) was used. The anode was the specimen, and the cathode was a stainless-steel plate. The duty cycle and the frequency were 20% and 2000 Hz, respectively, and the PEO treatment time was 4 min. The PEO electrolytic solution and resultant electrical parameters used above can obtain excellent corrosion resistance according to our previous work [10]. The fabricated PEO coatings were sealed with a polymeric sealant (Dichtol WFT Standard # 1532; Diamant Metallplastic GmbH, Mönchengladbach, Germany). The sealant was continuously brushed onto the PEO coatings surfaces for 5 min and then dried in the open air. In order to eliminate the influence of the resin layer on the sliding wear process, the coating after sealing treatment was ground on 1000 mesh and 1500 mesh sandpapers in order to ensure that the excess resin layer on the surface of PEO film was completely removed. The crosssection of the sealed PEO coating and the worn surfaces after wear tests were examined using a scanning electron microscope (FEI Quanta 200 F SEM, Eindhoven, the Netherlands), equipped with EDS. The dry sliding wear tests were performed using a ball-on-disk tribometer (HT-1000, Lanzhou ZhongkeKaihua Technology Development Co., Ltd., Lanzhou, China). A 5 mm-diameter Si₃N₄ ball was used as a counter body. The sliding velocity was 0.1 m/s. A series of loads (3N, 5N, 7N) were applied on the unsealed PEO coatings, and a series of loads (3N, 5N, 7N, 9N, 13N, 17N, 21N) were applied on the sealed PEO coatings.

3. Results and Discussion

The cross-sectional microstructure of the sealed PEO coating and the corresponding EDS mapping are presented in Figure 1.

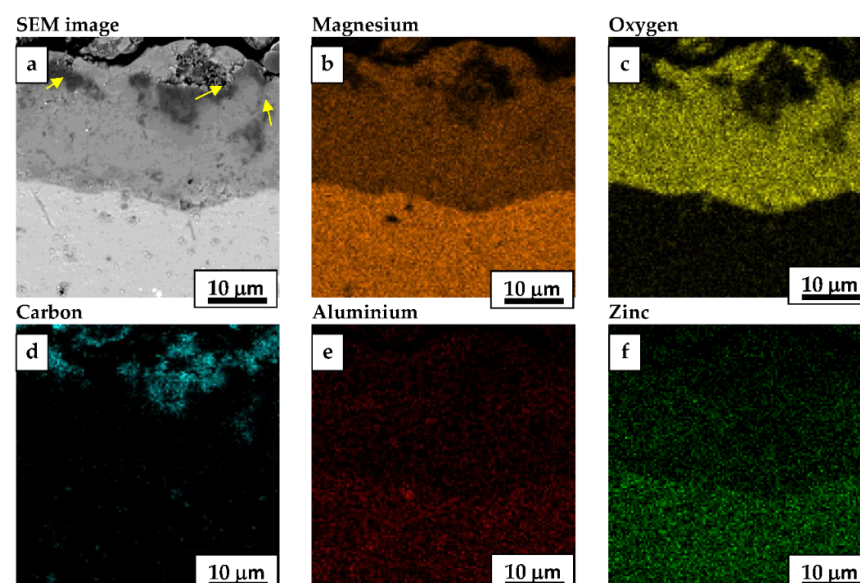


Figure 1. (a) The cross-sectional SEM image of the sealed PEO coating; (b–f) EDS mapping.

The Mg-based PEO coating fabricated in silicate electrolyte was mainly composed of MgO and Mg_2SiO_4 [8,10]. The darker areas in Figure 1a are the micropores and microcracks which originated from the PEO process, and these areas were mostly filled with the sealant. The distribution of carbon reflects the distribution of sealant (Figure 1d). It can be seen that the sealant efficaciously penetrated deep into the PEO coating, especially the porous top layer. The volume of the sealant at the top portion was much higher than that of the bottom portion of the coating. This can be attributed to the distribution of the intrinsic micro defects in the Mg-based PEO coating. There were open pores (arrows in Figure 1a) in the top area of the coating, which served as the ingresses for the sealant. The sealant penetrated through the open pores, filled the inter-connected micro defects, and solidified within them, thereby sealing the PEO coating.

The coefficient of friction (COF) curves and cross-sectional profiles of the wear tracks are presented in Figure 2.

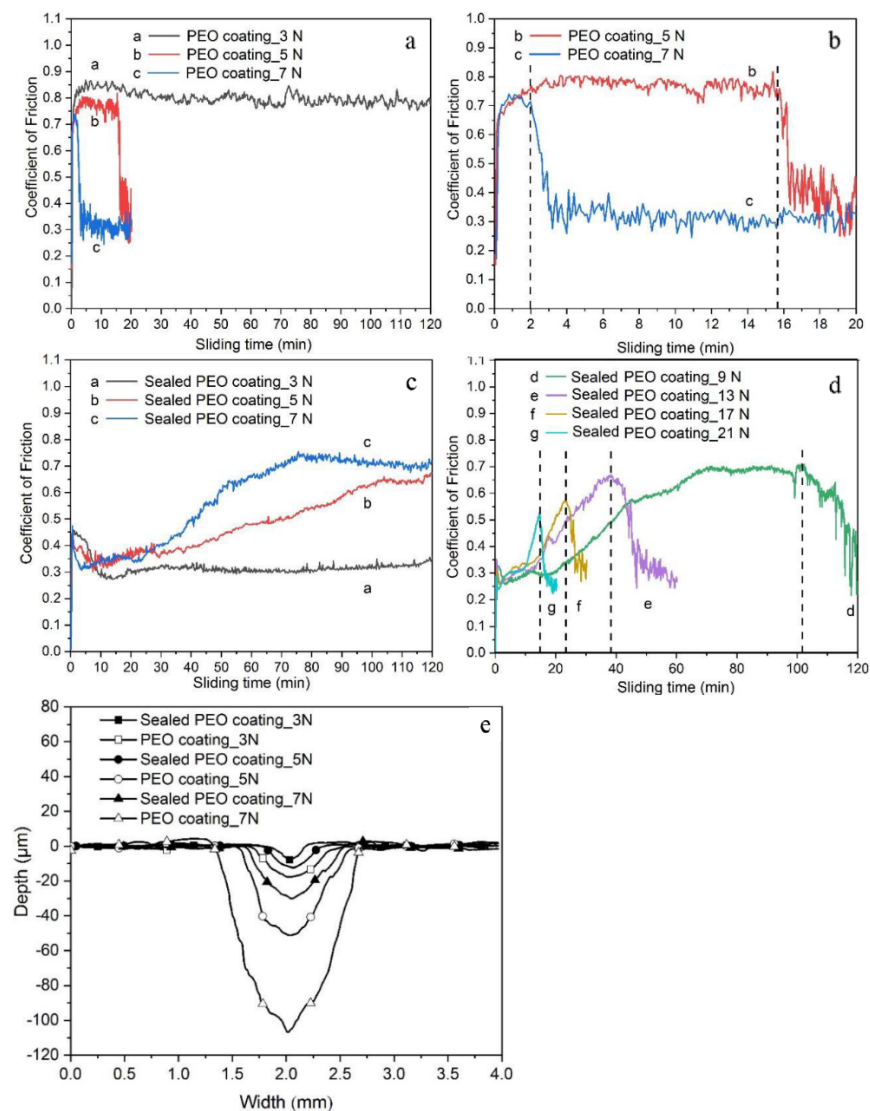


Figure 2. Coefficient of friction as a function of sliding time for (a,b) unsealed PEO coating; (c,d) sealed PEO coating and (e) cross-sectional profiles of wear tracks.

The dashed vertical lines in Figure 2b,d indicate the points of failure of the coatings, where the COFs decreased precipitously. When the applied load was at 3 N, the COF of the sealed PEO coating was much lower, and the curve was less scattered than the unsealed sample.

The calculated volumetric wear rates and the average COF of the samples are listed in Table 1.

Table 1. Wear rates and coefficient of friction of sealed and unsealed PEO coatings.

| Samples | Sliding Wear Rate (mm ³ /N·m) | Coefficient of Friction |
|-----------------------------|--|-------------------------|
| Sealed PEO coating at 3 N | 9.26×10^{-6} | 0.32 ± 0.03 |
| Unsealed PEO coating at 3 N | 3.43×10^{-5} | 0.80 ± 0.04 |
| Sealed PEO coating at 5 N | 1.39×10^{-5} | 0.48 ± 0.11 |
| Unsealed PEO coating at 5 N | 5.20×10^{-4} | 0.69 ± 0.16 |
| Sealed PEO coating at 7 N | 4.97×10^{-5} | 0.58 ± 0.16 |
| Unsealed PEO coating at 7 N | 1.34×10^{-3} | 0.36 ± 0.12 |

The SEM images of the worn surfaces are shown in Figure 3.

There were numerous intrinsic pores on the surfaces of the unsealed samples, which can be seen along with the wear tracks in Figure 3a,c. The polymeric sealant filled these kinds of pores in the sealed coatings, leading to the formation of smoother wear surfaces on them, compared to the unsealed samples. After a sliding distance of 720 m under 3 N load, the wear track of the sealed sample was much smaller than the unsealed sample. A large amount of sealant remnants can be found on the wear track as indicated by purple-colored areas in the EDS mapping result displayed in Figure 3b. The sealant in the top layer of the coating participated in the wear process, which effectively reduced the value of COF and the formation of severe cracks. This can be attributed to the apparent lubrication effect of the sealant, which was composed of polymer. The calculations showed that the sliding wear rate of the sealed coating was reduced to nearly one fourth of the value of the unsealed coating. When the applied load was increased to 5 N and 7 N, the unsealed PEO coatings broke at ~16 min and 2 min durations, respectively. The pre-mature failure of the unsealed coatings suggests that these coatings are ineffective for offering protection, even under mild wear regimes. Especially under 7 N, the rapid failure of the coating indicated that the load was much too high for the coating to bear, leading to the destructive delamination of the coating. However, the sealed coatings survived a two-hour sliding wear process under these loads. As shown in Figure 2c, the COF was at a low level during the initial 30 min, after which the COF steadily and slowly increased, and finally it stabilized between ~0.7 and ~0.65. The slow increase in the COF values corresponded well with the worn area ranging from the top layer to bottom layer of the coating, which also correlated with the gradational decrease in the volumetric distribution of the sealant. A very low quantity of sealant was found when the depth of the wear track was ~15 µm, as seen in Figure 3d, which indicated that the worn area was a sealant-starved bottom layer.

The survival time of the sealed coatings under further increase in axial loads (9, 10, 17 and 21 N) was also investigated. As presented in Figure 2d, when the load was higher, the failure of the sealed coating occurred earlier. During the initial 10 min sliding time, the wear track was not deep enough to reach the bottom layer; hence, the COF values of these samples were all between 0.25 and 0.35. After the sealant-rich top layer was worn off, the COF values and wear rate went up. It is worth noting that under the highest axial load of 21 N, the survival time of the sealed coating was close to the unsealed sample tested under a load of 7 N and longer than that of 5 N. The presence of the sealant significantly improved the load-bearing capacity of the PEO coating during sliding wear. Without the support of sealant, the porous brittle PEO coating was vulnerable to wear, especially under high loads. The intrinsic micro defects in the PEO acted as the nucleation spots for the generation of new cracks, which propagated under continuous impact of the counterbody [10,22]. This is evidenced by the severely cracked wear morphology observed in Figure 3a. There were splats surrounded by large-sized cracks on the wear track of the unsealed sample. If the wear process was allowed to continue further, then these isolated splats would become delaminated, similar to our observations made on thermal spray coatings [23,24].

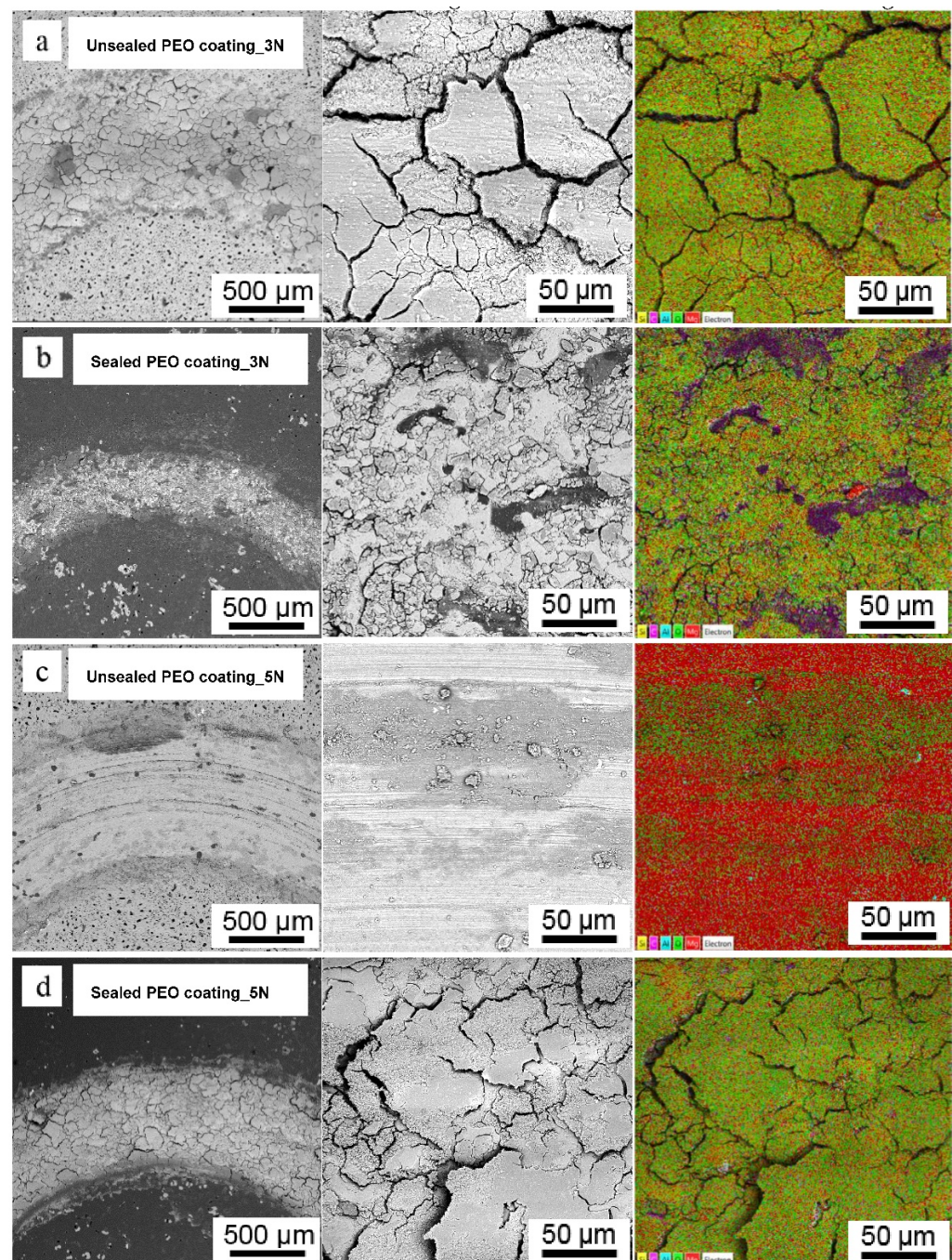


Figure 3. Wear morphologies of (a,c) unsealed PEO coatings and (b,d) sealed PEO coatings under loads of 3 N and 5 N.

4. Conclusions

The polymeric sealant was able to successfully penetrate into the PEO coating fabricated on the AZ31 Mg alloy, and it filled the microdefects. The sealed PEO coating showed a much lower volumetric wear rate than the unsealed PEO coating under low loads (3 and 5 N). While under relatively high loads, the unsealed PEO coating became delaminated and could not provide wear protection for the Mg alloy substrate. The presence of the sealant significantly improved the load-bearing capacity of the PEO coating during sliding wear, and the sealed coating survived for an extended period of time (15 min) under an extremely high load (21 N).

Author Contributions: Conceptualization, Q.W. and S.T.; methodology, Q.W. and Y.R.; software, Q.W. and R.C.S.; validation, Q.W., S.T. and Y.R.; formal analysis, Q.W. and R.C.S.; Investigation, Y.R. and S.T.; resources, Y.R.; data curation, Q.W., Y.R. and S.T.; writing—original draft preparation, Y.R., S.T. and R.C.S.; writing—review and editing, R.C.S., Q.W., S.T. and Y.R.; visualization, S.T.; supervision, Q.W.; project administration, Q.W.; funding acquisition, Q.W. All authors have read and agreed to the published version of the manuscript.

Funding: This work was financially supported by the Natural Science Foundation of Hunan Province (2019JJ40045) and the Changsha Science and Technology Project (No. kq 1801004).

Institutional Review Board Statement: Not applicable.

Informed Consent Statement: Not applicable.

Data Availability Statement: Data sharing is not applicable to this article.

Conflicts of Interest: The authors declare that they have no known competing financial interests or personal relationships that could have appeared to influence the work reported in this paper.

References

1. Pan, H.; Ren, Y.; Fu, H.; Zhao, H.; Wang, L.; Meng, X.; Qin, G. Recent developments in rare-earth free wrought magnesium alloys having high strength: A review. *J. Alloys Compd.* **2016**, *663*, 321–331. [[CrossRef](#)]
2. Riaz, U.; Shabib, I.; Haider, W. The current trends of Mg alloys in biomedical applications—A review. *J. Biomed. Mater. Res. Part B: Appl. Biomater.* **2019**, *107*, 1970–1996. [[CrossRef](#)]
3. Chaharmahali, R.; Fattah-Alhosseini, A.; Babaei, K. Surface characterization and corrosion behavior of calcium phosphate (Ca-P) base composite layer on Mg and its alloys using plasma electrolytic oxidation (PEO): A review. *J. Magnes. Alloys* **2021**, *9*, 21–40. [[CrossRef](#)]
4. Rao, Y.; Wang, Q.; Oka, D.; Ramachandran, C.S. On the PEO treatment of cold sprayed 7075 aluminum alloy and its effects on mechanical, corrosion and dry sliding wear performances thereof. *Surf. Coat. Technol.* **2020**, *383*, 125271. [[CrossRef](#)]
5. Luo, S.; Wang, Q.; Ye, R.; Ramachandran, C.S. Effects of electrolyte concentration on the microstructure and properties of plasma electrolytic oxidation coatings on Ti-6Al-4V alloy. *Surf. Coat. Technol.* **2019**, *375*, 864–876. [[CrossRef](#)]
6. Zeng, D.; Liu, Z.; Bai, S.; Wang, J. Influence of Sealing Treatment on the Corrosion Resistance of PEO Coated Al-Zn-Mg-Cu Alloy in Various Environments. *Coatings* **2019**, *9*, 867. [[CrossRef](#)]
7. Moon, S.; Arrabal, R.; Matykina, E. 3-Dimensional structures of open-pores in PEO films on AZ31 Mg alloy. *Mater. Lett.* **2015**, *161*, 439–441. [[CrossRef](#)]
8. Chen, Z.; Ji, H.; Geng, X.; Chen, X.; Yong, X.; Zhang, S. 3-D distribution characteristics of the micro-defects in the PEO coating on ZM6 mg-alloy during corrosion. *Corros. Sci.* **2020**, *174*, 108821. [[CrossRef](#)]
9. Zhang, Y.; Wang, Q.; Ye, R.; Ramachandran, C.S. Plasma electrolytic oxidation of cold spray kinetically metallized CNT-Al coating on AZ91-Mg alloy: Evaluation of mechanical and surficial characteristics. *J. Alloys Compd.* **2022**, *892*, 162094. [[CrossRef](#)]
10. Rao, Y.; Wang, Q.; Chen, J.; Ramachandran, C.S. Abrasion, sliding wear, corrosion, and cavitation erosion characteristics of a duplex coating formed on AZ31 Mg alloy by sequential application of cold spray and plasma electrolytic oxidation techniques. *Mater. Today Commun.* **2021**, *26*, 101978. [[CrossRef](#)]
11. Toorani, M.; Aliofkhaezraei, M.; Naderi, R.; Golabadi, M.; Aghdam, A.S.R. Role of lanthanum nitrate in protective performance of PEO/epoxy double layer on AZ31 Mg alloy: Electrochemical and thermodynamic investigations. *J. Ind. Eng. Chem.* **2017**, *53*, 213–227. [[CrossRef](#)]
12. Toorani, M.; Aliofkhaezraei, M.; Mahdavian, M.; Naderi, R. Superior corrosion protection and adhesion strength of epoxy coating applied on AZ31 magnesium alloy pre-treated by PEO/Silane with inorganic and organic corrosion inhibitors. *Corros. Sci.* **2021**, *178*, 109065. [[CrossRef](#)]
13. Castellanos, A.; Altube, A.; Vega, J.; García-Lecina, E.; Díez, J.; Grande, H. Effect of different post-treatments on the corrosion resistance and tribological properties of AZ91D magnesium alloy coated PEO. *Surf. Coat. Technol.* **2015**, *278*, 99–107. [[CrossRef](#)]
14. Ghanbari, A.; Attar, M. A study on the anticorrosion performance of epoxy nanocomposite coatings containing epoxy-silane treated nano-silica on mild steel substrate. *J. Ind. Eng. Chem.* **2015**, *23*, 145–153. [[CrossRef](#)]
15. Mingo, B.; Arrabal, R.; Mohedano, M.; Llamazares, Y.; Matykina, E.; Yerokhin, A.; Pardo, A. Influence of sealing post-treatments on the corrosion resistance of PEO coated AZ91 magnesium alloy. *Appl. Surf. Sci.* **2018**, *433*, 653–667. [[CrossRef](#)]
16. Liu, Y.; Wen, S.; Liang, G.; Tian, G. Improvement in corrosion resistance of micro-arc oxidized AZ91 alloy sealed with cement-mixed paraffin wax. *J. Mater. Res. Technol.* **2021**, *15*, 6956–6973. [[CrossRef](#)]
17. Van Phuong, N.; Fazal, B.R.; Moon, S. Cerium- and phosphate-based sealing treatments of PEO coated AZ31 Mg alloy. *Surf. Coat. Technol.* **2017**, *309*, 86–95. [[CrossRef](#)]
18. Li, L.-H.; Narayanan, T.S.; Kim, Y.K.; Kong, Y.-M.; Park, I.S.; Bae, T.S.; Lee, M.H. Deposition of microarc oxidation-polycaprolactone duplex coating to improve the corrosion resistance of magnesium for biodegradable implants. *Thin Solid Films* **2014**, *562*, 561–567. [[CrossRef](#)]

19. Zhang, S.; Li, Q.; Chen, B.; Yang, X. Preparation and corrosion resistance studies of nanometric sol–gel-based CeO₂ film with a chromium-free pretreatment on AZ91D magnesium alloy. *Electrochim. Acta* **2010**, *55*, 870–877. [[CrossRef](#)]
20. Zhu, J.; Jia, H.; Liao, K.; Li, X. Improvement on corrosion resistance of micro-arc oxidized AZ91D magnesium alloy by a pore-sealing coating. *J. Alloys Compd.* **2021**, *889*, 161460. [[CrossRef](#)]
21. Kim, H.-J.; Lee, C.-H.; Kweon, Y.-G. The effects of sealing on the mechanical properties of the plasma-sprayed alumina-titania coating. *Surf. Coat. Technol.* **2001**, *139*, 75–80. [[CrossRef](#)]
22. Takadoum, J. *Materials and Surface Engineering in Tribology*; Wiley: Hoboken, NJ, USA, 2008.
23. Wang, Q.; Ramachandran, C.S.; Smith, G.M.; Sampath, S. Sliding wear behavior of air plasma sprayed Al₂O₃ coatings sealed with aluminum phosphate. *Tribol. Int.* **2017**, *116*, 431–439. [[CrossRef](#)]
24. Ramachandran, C.; Balasubramanian, V.; Ananthapadmanabhan, P.; Viswabaskaran, V. Understanding the dry sliding wear behaviour of atmospheric plasma-sprayed rare earth oxide coatings. *Mater. Des.* **2012**, *39*, 234–252. [[CrossRef](#)]